ICAS 2016
30th Congress of the International Council of the Aeronautical Sciences
DCC, Daejeon, Korea ; September 25-30, 2016

EFFECTIVENESS OF VORTEX GENERATORS IN HIGHLY 3D FLOWS

H S Mudhar*
***City University London**

Keywords: *swept wings, turbulent boundary layer, vortex generators*

Abstract

An experiment was carried out in the T2 wind tunnel at the Handley Page Laboratory, aiming to explore the effectiveness of vortex generators (VGs) in controlling turbulent separation at the rear of a highly swept (60°) wing. Three sets of triangular vane vortex generators were tested with heights, h_v of 5, 10 and 16mm. These VGs allowed for a parametric study involving their orientation to the local flow β, spanwise spacing, D and δ/h_v. The effectiveness of the VGs was judged by their ability to suppress the boundary-layer separation with a minimal drag penalty. Flow visualization and Laser Doppler Anemometry measurements showed an optimum orientation β of 30° with a spacing ratio D/h_v of 12 where VGs with height half the boundary-layer thickness were able to fully prevent the separation.

1. Introduction

Flow separation and its control remain one of the most important aspects in aircraft performance improvement.

Flow separation is one of the most significant boundary-layer phenomenon which has a number of adverse effects including loss of lift and increase of drag. The aim of separation control is to influence the flow in a way to reduce the mean reverse flow or even eliminate it completely [1].

Flow control devices come in many forms but can be classified either as active or passive. Active flow control involves the use of external energy through blowing air or moving surfaces. On the other hand passive flow control requires no external energy and of these the simple vane VGs are among the most well-known. Today flow control using passive devices is the cheapest and fastest solution to implement [2].

VGs operate on a simple mechanism of momentum transfer. The VGs are appropriately shaped and orientated to the local flow to produce a small wingtip vortex which entrains high momentum flow from closer to (or within) the freestream into the low momentum boundary-layer flow. This process is known to re-energize the boundary layer and hence enables it to travel further against an adverse pressure gradient before separating.

For aircraft, the problem caused by flow separation at high lift coefficients has been at the forefront of aerodynamic advances for a number of years. Being able to operate at a higher C_L value without incurring flow separation allows for a number of benefits especially during maneuvers where the wing is at a high angle of attack such as during landing and take-off. Delaying flow separation through the use of VGs has similar benefits to other flow control devices in that they allow for increase in maximum rate of climb and maximum lift, whilst reducing the take-off run, approach speed and stall speed.

VGs have been rigorously investigated over a number of years ever since experiments from Taylor [3] where they were used to eliminate diffuser separation and control airflow in wind tunnel diffusers and demonstrated their capabilities to control boundary-layer flow. Today they are known to have a number of applications in flow control and be seen on a number of aircraft such as the Boeing 737, the Harrier and a number of light aircraft. Despite this their effectiveness in highly three-dimensional (3D) flows, such as those experienced by highly swept wings (Λ>40°) is unclear. Research in this area is scarce despite

the aerodynamic benefits achievable. Highly swept wings are common on high speed aircraft such as fighter aircraft where the delay of shock-formation is more important and low speed stability is sacrificed. Typical airliners employ a moderate sweep where the 3D effects are lower and some low speed stability is required.

Over the years a few studies have been conducted to look into the effectiveness of VGs on highly swept wings. Pearcy [5] realised in 1961 that a suitably positioned co-rotating array of vortex generators may be used to control the crossflow associated with swept wings. These guidelines were followed in subsequent tests and used to delay flow separation on modern moderate swept planes such as the ERJ-145, Boeing 737 and also the new Boeing 777-300 ER [4].

In 1995, Langan and Samuels [6] conducted a wind-tunnel test into the effectiveness of a set of co-rotating vanes on a 40^o leading edge diamond wing model. The experimental tests focused on manoeuvre performance enhancements on advanced fighter/attack aircraft and were tasked with enhancing the manoeuvre and control capability of the next generation Air Force fighter aircraft. Various types of VGs and array types were tested and results were gathered through surface pressure measurements and flow visualisation in order to characterise the separation lines. The results showed that all vortex generators tested showed improvement (up to 5%) in manoeuvre L/D with flaps at LE=20°, TE=0°. The same VGs degraded performance, in all but a few cases, with flaps at LE=15°, TE=10°. The experiment focused more on the manoeuvre characteristics in terms of lift and drag rather than separation control. The model being tested was also only swept at 40^o at the leading edge with a diamond shape, which is considerably less the some aircraft which use a conventional wing with a sweep of 60^o in some cases. Flow phenomenon will be different in both cases

Ashill [7] provides interesting flow control applications on highly swept wings using sub-boundary layer (low-profile) vortex generators. The experiments took place in the 13ft x 9ft Wind Tunnel at DERA, Bedford, on 60^o leading-edge sweep delta wing models at a freestream Mach number of 0.18 and a Reynolds number on geometric mean chord of $4x10^6$ [8] . However the VGs were placed at the leading edge of the model in order to counter the leading edge separation line rather than separation at the trailing edge region.

More recently Broadley [9] conducted wind tunnel investigations into low subsonic flow characteristics of highly swept wings ($\Lambda = 30^o$ to 60^o) and the use of VGs to control the associated flow separations over the upper surface in the region of the trailing edge. The experiment was performed on two half model wings in two different wind tunnels (Cranfield University and DERA Bedford) to determine the effectiveness of vane VGs in controlling the turbulent separation at the trailing edge of a highly swept wing. Cropped delta VGs were used on swept wings to investigate the effects of chordwise position vane size, vane orientation and spanwise spacing on separation control. Results showed that upright cropped delta vane VGs were able to effectively control separation on highly swept wings up to 60^o and a set of design guidelines for optimum performance was set. However these guidelines were not complete as the number of vortices per unit length was not investigated fully to determine whether the efficiency depended on a minimum number of vortices per unit length for all sizes of vortex generator or just the spacing of the VGs. The oil visualisation and pressure measurements also proved to be inadequate for determining the nature of the flow behind the separation line so detailed measurements using optical techniques were recommended to understand the physics and characterise the VG induced flow over a swept wing.

To address the questions posed above; this paper reports the results of an experiment looking into the effectiveness of passive vane VGs in controlling the turbulent separation at the rear end of a highly swept (60^o) wing, with a thick aerofoil (NACA0050). The work was performed to optimise the VGs parameters and set a number of guidelines for effective flow control. Once the VGs are optimised, detailed optical measurements downstream of the VGs are to help understand the mechanisms by which

a row of co-rotating VGs prevent flow separation.

Recently, optical techniques such as LDA and Particle Image Velocimetry (PIV) have been used to investigate the vortex dynamics and physical mechanisms involved in the process of separation control using VGs. Angele and Grewe [10] investigated the development of streamwise vortices from VGs in adverse pressure gradient (APG) separation using PIV. The development of the vortical structures from the counter-rotating vanes was mapped downstream of the VGs through vortex strength and vorticity. Similar experiments were carried out by Tilman and Langan [11] where LDA was used to investigate the development of vortex paths and vortex decay using VGs of various types in zero-pressure gradient flow and counter rotating VGs in an APG. Velte, Hansen and Cavar [12] [13] also looked at the flow analysis of VGs on wing sections by stereoscopic PIV measurement on a bump with counter–rotating array.

These experiments however do not help understand the mechanisms of flow control by a row of co-rotating VGs on a swept wing and this is one of the main aims of this study.

2. Experimental Set-Up

2.1 Model and Wind Tunnel

The model used during the experiment was wooden with a NACA0050 aerofoil profile swept by 60° with three sets of 50 pressure tappings on both the port and starboard sides. This was chosen as it was expected to produce highly three-dimensional flows and also generate a good region of separated flow at the rear end of the model due to the strong adverse pressure gradient. It was mounted between the floor and ceiling of the test section of the T2 low speed (4-55 m/s) wind tunnel at the Handley Page Laboratory, City University London at a zero-lift condition.

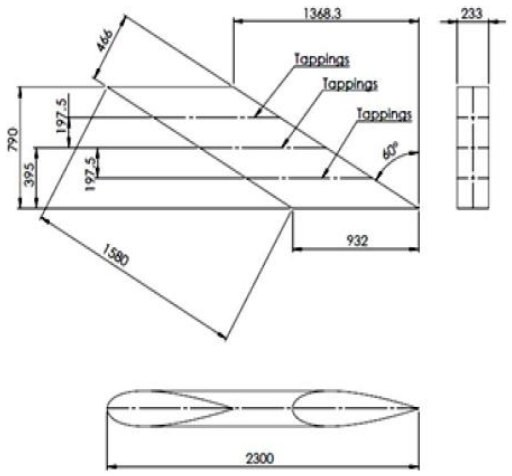

Fig 1: GA drawing of the experimental model

2.1 Baseline Tests

In order to design the VGs and decide where to place them it was necessary to conduct some bassline tests on the model in order to identify the thickness of the boundary layer as well as the location of flow separation and the local flow angles.

The three dimensional model was equipped with three equally-spaced spanwise stations of surface mounted pressure tappings with an internal diameter of 0.5mm (as shown in fig. 1) to measure the local static pressure. Each chordwise station contained 50 tappings. Simultaneous pressure measurements were achieved using a computerised pressure measurement system where the pressure tappings were connected to a 64-channel array of ESP-64HD miniature electronic pressure transducer equipped with integrated DTC (Digital Temperature Compensation) which allowed for in-situ calibrations using the factory calibration data stored in a built-in EEPROM and A/D converter. The pressure scanners rated at 2:5psig were interfaced to a CANdaq acquisition system with a choice of CAN, Ethernet or RS232 output that can be connected to a PC for data acquisition and processing using software provided by Aerotech.

This characteristic of the model allowed it to be aligned by balancing the pressure distributions on both sides of the model, ensuring that the attachment line was right at the

leading of the model (x=c = 0:0). Once the model was aligned the pressure distributions were acquired for flow speeds of 25m/s and 35m/s with Reynolds numbers (Re) of 1.54 million and 2.16 million respectively using the tappings S at mid-span.

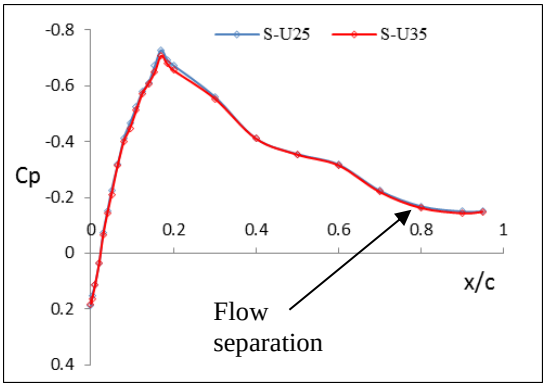

Fig 2: Pressure distributions along the clean model at Re of 1.54 million and 2.16 million at tapping station S where U25 is a freestream velocity of 25m/s.

Fig 2 indicates that flow separation occurs around x/c 0.8 and also shows that the pressure distributions at the two Re values are almost identical. In order to orientate the VGs appropriately, the local flow angles along the model (where the VGs are to be placed) needed to be found. To do this an 'ink-dot' technique was employed; this involved covering an A3 tracing paper with blue permanent marker dots at regular intervals and wrapping it around the model. This tunnel was the run at low speed and a spray gun was used to cover the paper with methyl salicylate. Once covered, the tunnel was taken up to the appropriate Re and each dot trailed a streak of ink which helped identify the local flow angles. It was challenging to apply this method on a vertical model as any slight overdose would result in the ink simply dripping down and a lack of liquid would not produce any streaks. This was why this method was not chosen for further tests as it was too time consuming but repeating the same case more than once then merging the 'good' regions on Adobe Photoshop where the presentable helped to give an accurate representation of the local flow angles as shown in fig 3. *(The streaks are shown in red rather than blue for visual purposes).*

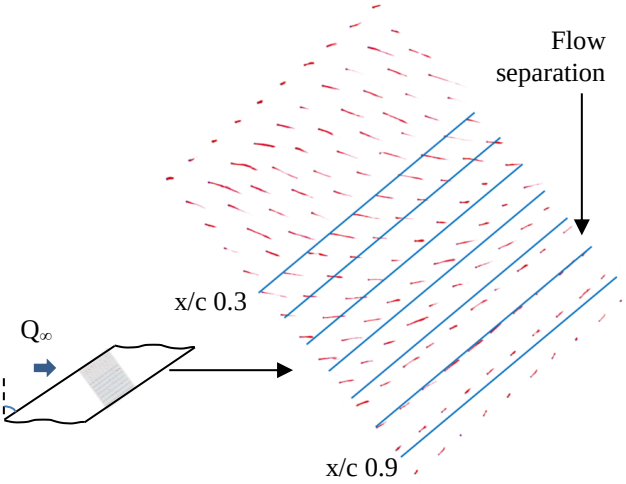

Fig 3: Ink-dot flow visualisation over the clean model

Fig 3 also helps to identify the location of flow separation at around x/c 0.8 when the local flow is completely aligned with the spanwise direction; this confirms findings from fig 2. The local flow angles are summarised in the Table 1.

x/c	0.3	0.4	0.5	0.6	0.7	0.8	0.9
α (°)	-20	-10	-5	5	20	30	30

Table 1: Local flow angle values relative to the freestream flow direction (where 0° is the freestream direction and 30° is fully spanwise flow)

Since the VGs were to be placed prior to separation and in the APG, the boundary layer thickness in this region was needed to help scale the height of the VGs. The boundary layer measurements were then taken using a pitot rake and aligning it in the direction of the local streamline direction. The streamline direction at each boundary layer measurement location was taken from Table 1 and the rake was aligned accordingly.

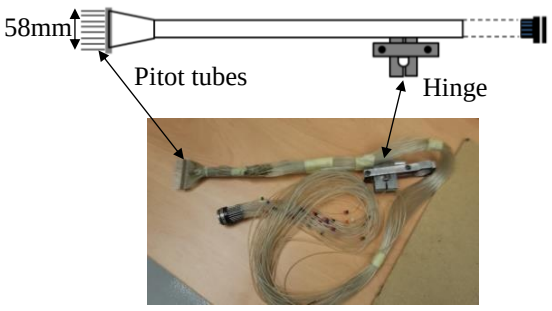

Fig 4: Schematic and photographic representation of the Pitot rake used for boundary layer measurements

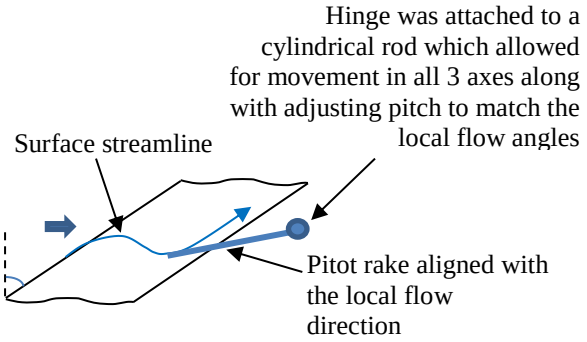

Fig 5: Schematic representation of the Pitot rake

The boundary layer thicknesses were 5.5mm at x/c 0.3, 7mm at x/c 0.4, 10mm at x/c 0.5 and 13mm at x/c 0.6 for both Re.

2.2 Design and Arrangement of VGs

Three sets of triangular vane VGs were manufactured with the dimensions shown in Table 2.2. The VGs were designed to cover a wide range of δ/h values to include configurations where the ratio was below, above and equal to one. A thin (0.5mm) sheet of aluminium was used to manufacture the VGs; the thickness was based on the ESDU guide [14] which suggests that the ratio of l_v/t_v where t_v is the thickness should be 0.05 or less.

	VG 1	VG 2	VG 3
Height (mm), h_v	16	10	5
Length (mm), l_v	32	20	10
Flange Width (mm)	10	6	3
l_v/t_v	0.016	0.025	0.050

Table 2: VG parameters

In accordance with the literature [9], the VGs were placed in a toed-out co-rotating array, and attached to the model using thin double sided tape.

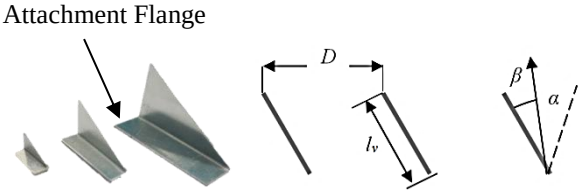

Fig 6: Image of the three different VG sizes used (left) and the plan view of the arrangement of the VGs in a co-rotating array where *D* is the spanwise distance between adjacent VGs and *β* is the orientation of the VG to the local flow (right)

3. Results

Initially a fixed spanwise spacing *D* was chosen as 125mm while varying the orientation, chordwise location and VG height. This was slightly more than the spacing chosen by Broadly [9] of 80mm.

h_v (mm)	16			10			5		
x/c	0.3	0.4	0.5	0.3	0.4	0.5	0.3	0.4	0.5
δ/h_v	0.3	0.4	0.6	0.6	0.7	1.0	1.1	1.4	2

Table 3: Range of δ/h_v tested.

The VGs were tested at three chordwise locations which in turn gave a larger test space to investigate the δ/h_v parameter effect on separation control but also analyse the effects of chordwise location. Broadly [9] found that the VGs work better close to the separation line (5% chord upstream of separation) unlike those from the ESDU guidelines [15] which recommend positioning further upstream. Placing the VGs further upstream in the thinner boundary-layer would allow for the smaller VGs to bring in higher momentum flow but also be further from the separation line which may cause the vortex to decay considerably before reaching the separated regions. However since aircraft VGs need to have a wide operating area and the separation line would move forward when the wing generates lift, a study from x/c 0.3 to x/c 0.5 was conducted.

With a fixed x/c and *D* the orientations of the VGs to the local flow (angle *β*) were varied between 10° - 40°. The results from the flow visualisation indicated an optimum orientation of between *25-30°*, below which the vortex formed was significantly weaker and above which no additional benefit was noticeable.

Fig 7 shows how the orientation of the VGs is crucial in producing an adequate vortex to 'pull' the flow away from the spanwise direction and re-energise the chordwise component of the flow to control the 3D separation.

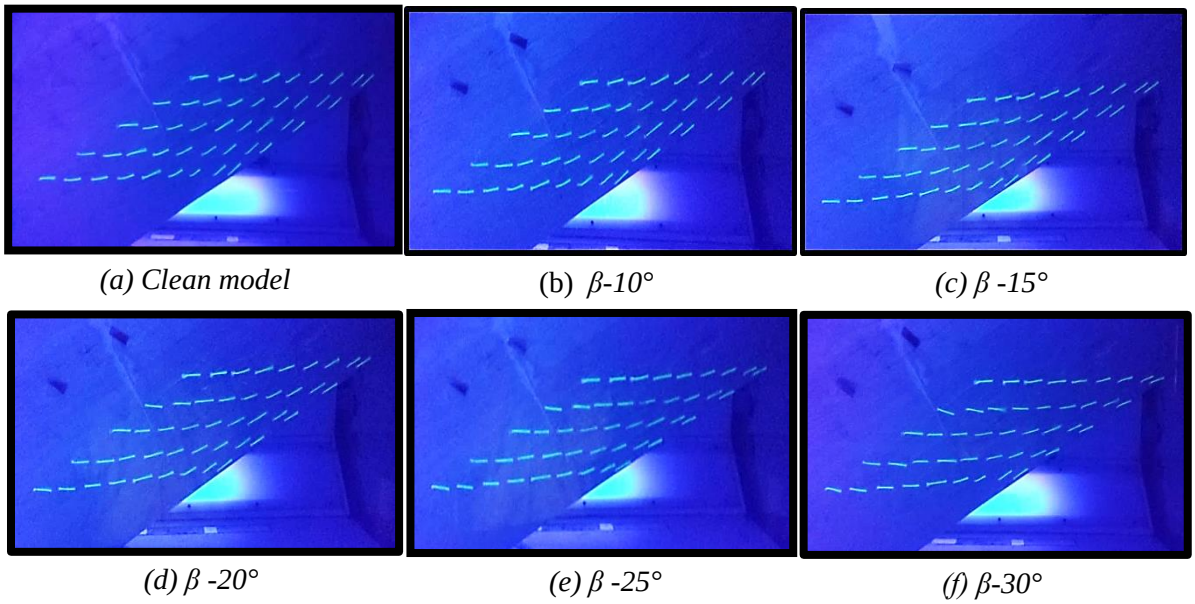

(a) Clean model (b) *β-10°* *(c) β -15°*

(d) β -20° *(e) β -25°* *(f) β-30°*

Fig 7: Tuft flow visualization using VGs with h_v of 16mm, *D* of 125mm at x/c 0.4 and *Re* 2.18 m.

A minimum orientation of 25° was found for all cases (x/c and h_v) using the flow visualization. However to fully evaluate the effectiveness of the VGs the drag penalty must also be accounted for. To get a measure of the drag on the model a single component DANTEC LDA system was used to obtain measurements in the wake as shown below:

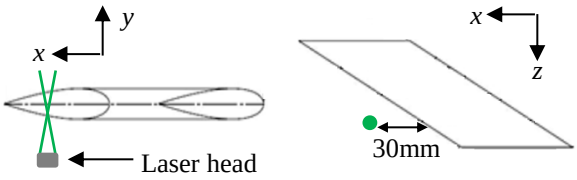

Fig 8: Schematic of LDA set-up

The results from the wake measurements are shown in fig 8. The results indicate a significant reduction in the size of the wake as the orientation angle of the VGs increased, this also confirms the trend in fig 7 where the flow tends to be fully attached at *β=30°*. However with further increase in orientation angle two distinct troughs appeared on each side of the wake profile which shows the excrescence drag of the VGs.

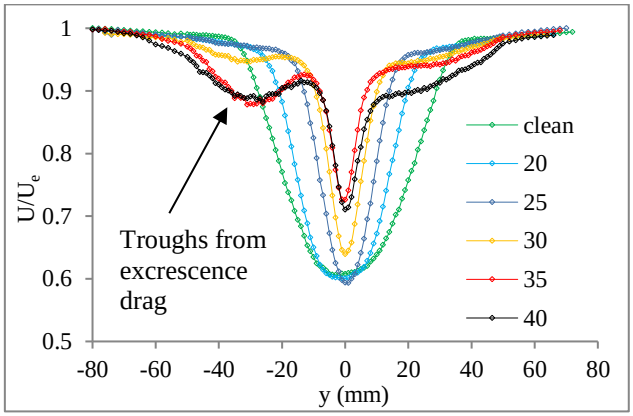

Fig 9: Comparison of the dimensionless U-mean velocity component variation across the wake of the model 30mm behind the trailing edge, with the VGs D/h_v 12 at x/c 0.5 and h_v=16mm using a single component LDA set up at Re of 2.18mil.

The drag on the model was calculated using a simple momentum equation. Since the transverse velocity component was unavailable, a simple 2D approach was taken. Using the continuity equation:

$$\dot{m}_{in} = \dot{m}_{out} \rightarrow \dot{m}_1 = \dot{m}_2 \rightarrow \rho u_1 b h_1 = \rho b \sum_{wake} u_2 \delta y \quad (1)$$

Using the momentum equation, where *Dr* is the drag, u_1 is the freestream velocity and c is the chord length of the model:

$$F_x = -Dr = \dot{M}_{x,out} - \dot{M}_{x,in} \quad (2)$$

$$\therefore Dr = -\left[\rho b \sum_{wake} u_2^2 \delta y - \rho b h_1 u_1^2\right] \quad (3)$$

$$\therefore Dr' = \frac{Dr}{b} = \rho h_1 u_1^2 - \rho \sum_{wake} u_2^2 \delta y \quad (4)$$

$$\therefore Dr' = \rho \sum_{wake} u_2 (u_1 - u_2) \delta y \quad (5)$$

Using continuity, momentum can be re-written as:

$$Dr' = \rho \left[\frac{\sum_{wake} u_2 \delta y}{u_1} u_1^2 - \sum_{wake} u_1^2 \delta y\right] \quad (6)$$

The following formula was used to calculate the drag coefficient:

$$C_D = \frac{Dr'}{\frac{1}{2}\rho u_1^2 c} \quad (7)$$

Due to the proximity of the measurements to the trailing edge of the model, the momentum deficit in different cases was represented as a percentage of total drag. This is probably a reasonable approach as a far-wake traverse would be influenced by change in pressure gradients caused by the reduction in wake blockage behind the model.

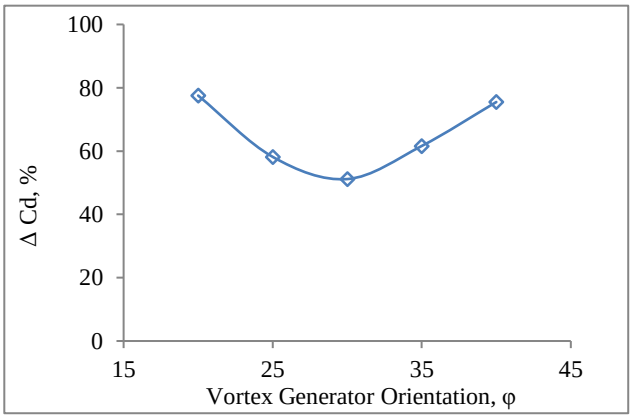

Fig 10: Percentage change of total drag compared to the clean model using VGs with h_v =16mm, δ/h_v=0.63 and D/h_v = 7.8 at *Re* of 2.18mil

Once it was found that the optimum orientation of the VGs was β=30°, a process of optimising the dimensionless spanwise spacing D/h_v at x/c of 0.5. The recommendations from ESDU [14] were followed, i.e. to choose a spacing ratio which allowed for subsequent tests to be conducted by simply adding or removing adjacent vanes. A range of D/h_v values were tested from 6 to 24 with increments of 6.

Fig 11 shows how reducing the spanwise spacing improves the separation control. Here δ/h_v=0.63. Using D/h_v 24 large regions of separated flow are present (although less than the clean model) with only the tufts directly in the wake of one of the VGs able to refrain from being pulled completely in the spanwise direction. Decreasing the spacing to D/h_v of 12 however allows for much greater control and all the regions are able to withstand the large crossflow component of flow although naturally the tufts at the trailing edge being to align to the spanwise direction due to the Kutta condition.

Similar trend can be seen in fig 12 where sub-boundary layer VGs with δ/h_v=2 were used. With D/h_v 12 full separation control was achieved but once again by increasing the value to D/h_v of 18 flow separation in the form of a separation line around x/c 0.9 is present.

Fig 13 compares two cases with D/h_v of 18 with the clean wing. It can be seen that although neither configuration prevents separation completely, the case with δ/h_v=1 works slightly better than δ/h_v=0.63. This can be attributed to the fact that although the VGs used for the δ/h_v=0.63 case are bigger than those used for δ/h_v=1, both are more or less bringing in similar momentum from the freestream but the greater spacing between the larger VGs causes larger pockets of separated flow to emerge.

The results from the spanwise spacing optimisation are summarised in fig 14. A similar wake analysis to the one in fig 9 was performed by changing the height of the VGs. Using the optimised cases of D/h_v 12; it was performed to distinguish whether certain configurations once again are hindered by a large drag penalty. The results from fig 15 show how the larger VGs produce large troughs of excrescence drag similar to that seen when β exceeds 30° in fig 9.

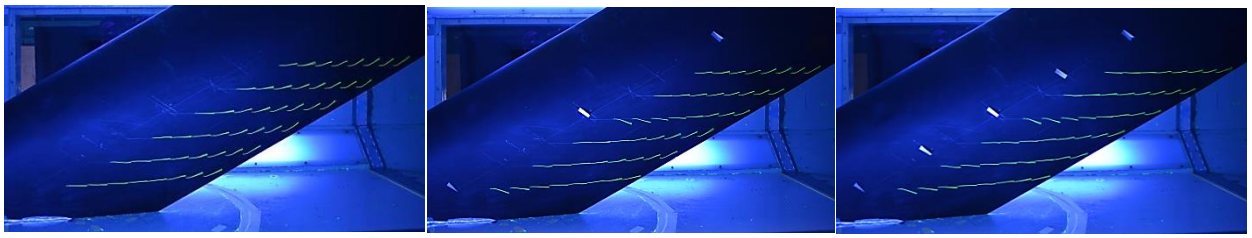

Fig 11: Flow visualisation over the rear end of the model using fluorescent tufts and UV lighting comparing the clean wing (left), D/h_v 24 (centre) and D/h_v of 12 (right) with $\delta/h_v=0.63$ at x/c 0.5 and $\beta = 30°$

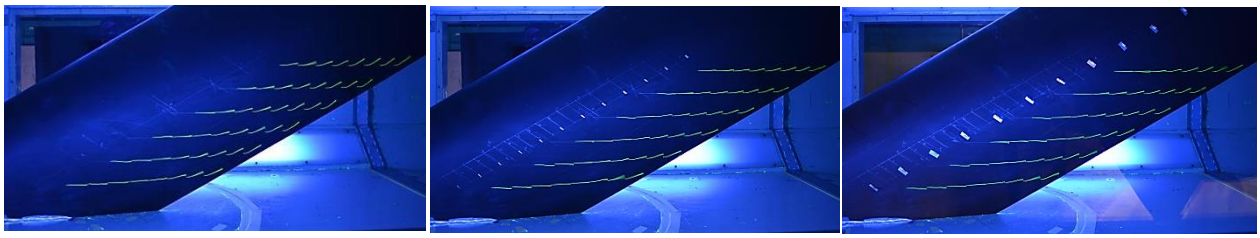

Fig 12: Flow visualisation over the rear end of the model using fluorescent tufts and UV lighting comparing the clean wing (left), D/h_v 12 (centre) and D/h_v of 18 (right) with $\delta/h_v=2$ at x/c 0.5 and $\beta=30°$ *(note that the VGs appear larger on the right image as extra tape was used to avoid detachment of VGs while using the LDA for long runs)*

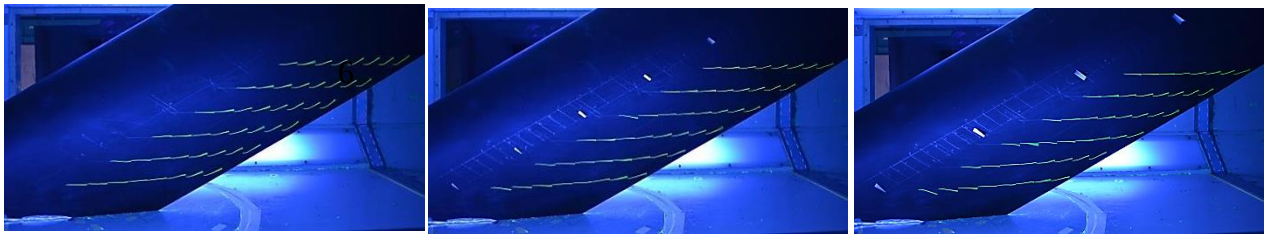

Fig 13: Flow visualisation over the rear end of the model using fluorescent tufts and UV lighting comparing the clean wing (left), $\delta/h_v=1$ (centre) and $\delta/h_v=0.63$ (right) with D/h_v 18 at x/c 0.5 and $\beta = 30°$.

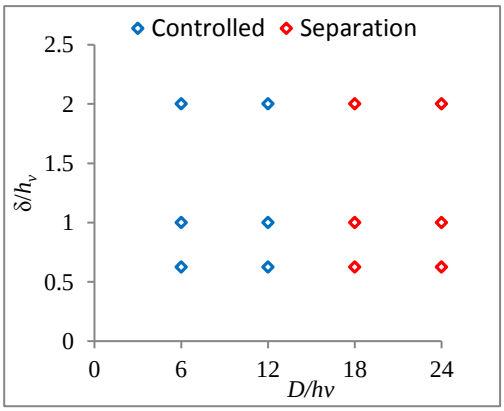

Fig 14: Test matrix and results from the spanwise spacing optimisation with x/c 0.5 and $\beta = 30°$ at *Re* of 1.54mil.

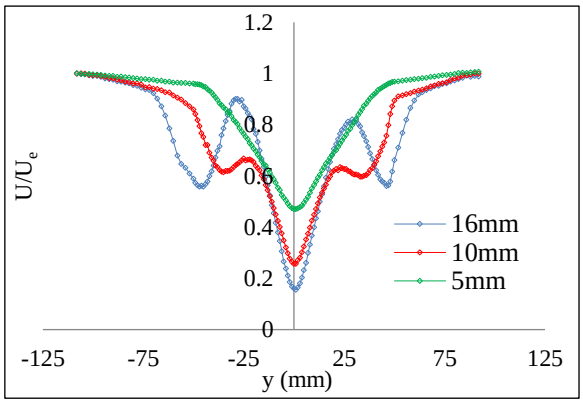

Fig 15: Comparison of the dimensionless U-mean velocity component variation across the wake of the model 30mm behind the trailing edge, with the VGs D/h_v 12 at x/c 0.5 and $\beta = 30°$ using a single component LDA set up at *Re* of 1.54mil

4. Discussion

It is evident from the flow visualization and the LDA measurements that an optimum configuration is achievable using passive vane VGs to fully suppress the turbulent boundary layer separation on a highly swept wing with highly 3D flows. The results show that small alterations of VG orientation, spanwise spacing and height can improve their performance both in terms of separation control and drag reduction. Fig 7 shows how a minimal orientation of the VG to the local flow is needed to produce a vortex with enough strength to re-energize the boundary layer. It was found that a minimal orientation of around 30° was needed for complete control. This value remained relatively constant over a range of flow conditions and also while changing the chordwise location or height of the VGs. This value is at the top end of the range, suggested by Broadly [9], of 18-30°.

Fig 10 shows how an optimal orientation can be found through wake measurements to assess the drag penalty of the VGs. At $\beta=20°$ the drag on the model is around 20% lower than that of the clean wing. This value continues to increase with increasing orientation until an optimum value at β=30° is found where the drag is half that of the clean wing. Beyond this orientation the drag being to build up again in a symmetrical fashion about β=30°. This phenomenon can be explained with reference to fig. 9 where the wake profiles reduce in size as the orientation increases and the separation line is pushed further downstream. However the excrescence drag created by the VGs become visible on the wake profile. Further increasing the setting angle of the VGs continues to reduce the size of the wake but in turn the VG wakes become significantly large due to the nature of the flow around the VGs, which begin to behave as bluff bodies on top of the model so their drag becomes more evident.

Once the orientation is increased above 35° the wake profile becomes slightly asymmetrical with a slightly larger vortex imprint on one side of the model due to the 3D nature of the flow.

The flow visualization from fig 11-13 shows how the effects of spanwise spacing are crucial in maintaining attached flow over the wing. The vortices from large spaced VGs configurations are susceptible to being overcome by the large crossflow velocity components on the swept wing. It is evident that the larger VGs ($\delta/h_v=0.63$) produce stronger vortices as the tufts directly in their wake are pulled down to oppose the spanwise flow. This is not visible on the smaller VGs despite all being at the same orientation. The results show that the more VGs there are, the greater the region of attached flow. After a parametric study of the spanwise spacing it became evident that a minimal spanwise spacing of around D/h_v of 12 was desirable. This was not investigated by Broadly [9] who maintained a spacing of 80mm which provided a D/h_v of 8. The spacing ratio of 12 was constant regardless of VG height, therefore a LDA wake analysis was performed and the results in fig 15 show how a similar phenomenon was witnessed to fig 9 where there imprints of the vortices from certain configuration the VGs are visible in the wake. In this case the largest VGs have the largest imprints which will add to the total drag on the model. The sub-boundary are VGs which are submerged within the boundary layer show no signs of this while maintaining separation control.

5. Conclusions

The results from a combination of flow visualisation and wake measurements have enabled an optimisation of the VGs to supress the turbulent boundary layer separation on a highly swept wing with strong 3D flows.

The results show that a number of parameters such as the VG orientation, spanwise spacing and height are key in maintaining attached flow.

A parametric study involving the local orientation, chordwise location, height relative to the local boundary thickness and spanwise spacing have allowed some insight into the effective parameters required to optimise a set

of passive co-rotating VGs on a highly swept wing.

δ/h_v	D/h_v	$\beta(°)$
2	~12	30

Table 4: Optimal parameters of VGs

A three-component LDA set-up is currently being used to take measurements along the span of the model downstream of the VGs. The two cases being analysed are listed:

(a) D/h_v 18, $\delta/h_v=2$, *x/c 0.5*

(b) D/h_v 12, $\delta/h_v=2$, *x/c 0.5*

These are being analysed as they have been found to be the optimum case and form the boundary between 'working' and separation in terms of the spanwise spacing with all other parameters constant. This will give indications into the physical mechanisms that help the VGs to control turbulent flow separation and help to characterise the vortex induced flow in terms of its strength and decay.

References

[1] C. Kuzuguden, D Erdem, *"Passive control of a turbulent boundary layer under adverse pressure gradient"* AIAC-2015-099, 2015.

[2] H. Tebbiche, M.S. Boutoudy, "*Optimized vortex generators in the flow separation control around a NACA 0015 profile"* 2311-9020, 2014.

[3] Taylor, H. D. "*Summary report on vortex generators*". Research Department Report No. R-05280-9. United Aircraft Corporation, East Hartford, Connecticut, 1950

[4] Thomson K and Schulze E T, "*Delivering fuel and emission savings for the 777*", QTR_03, 2009.

[5] Pearcey, H. H., "*Shock-induced separation and its prevention by design and boundary layer control".* In: 'Boundary Layer and Flow Control, its Principles and Applications Vol. 2, Edited by G. V. Lachmann, Pergamon Press, Oxford, 1961.

[6] Langan KJ, Samuels JJ. "*Experimental investigation of manoeuvre performance enhancements on an advanced fighter/attack aircraft*". AIAA Paper 95-0442, AIAA 33rd Aerospace Sciences Meeting, Reno, NV, January 9–12, 1995

[7] Ashill PR, Riddle GL, Stanley MJ. "*Control of three-dimensional separation on highly swept wings".* ICAS-94-4.6.2, September 1994.

[8] John C Lin, "*Review of research on low-profile vortex generators to control boundary-layer separation".* Flow Physics and Control Branch, NASA Langley Research Centre, Hampton, VA 23681-2199, USA, Progress in Aerospace Sciences, Volume 38, Issues 4–5, May–July 2002, Pages 389–420.

[9] Broardly J I, "*the control of trailing edge separation on highly swept wings using vortex generators,*" Total technology PhD, College of Aeronautics, Cranfield, UK. October 1998

[10] K. P. Angele, F. Grewe, "*Investigation of the development of streamwise vortices from VGs in ARPG separation using PIV",* Department of Mechanics, Stockholm, Sweden.

[11] C P Tilman, J K Langan, "*Laser Doppler Anemometry Investigation on Sub Boundary Layer Vortex Generators for flow control*" DERA Bedford, UK, 2000.

[12] C. M. Velte, M O L Hansen, D Cavar "*Flow analysis of VGs on wing sections by stereoscopic PIV*", Fluid Mechanics, Department of Mechanical Engineering, Technical University of Denmark, 2007.

[13] C. M. Velte "*Characterization of VG induced flow*", Fluid Mechanics, Department of Mechanical Engineering, Technical University of Denmark, 2009.

[14] "*Vortex generators for control of shock-induced separation*", part 2 guide to use of vane vortex generators, ESDU, 93025

[15] "*Vortex generators for control of shock-induced separation*", part 1 introduction and aerodynamics, ESDU, 93024

Contact Author Email Address

harcharan.mudhar.1@city.ac.uk

Copyright Statement